PROCEEDINGS OF SCIENCE

The GAPS Time-of-Flight Detector

Sydney Feldman[a,*] **for the GAPS collaboration**

[a] *Dept. of Physics and Astronomy, University of California*
Los Angeles, CA, 90095 USA

E-mail: sydneyfeldman@physics.ucla.edu

The General Antiparticle Spectrometer (GAPS) Antarctic long duration balloon mission is scheduled for launch during the austral summer of 2024-25. Its novel detection technique, based on exotic atom formation, excitation, and decay, is specifically designed for the detection of slow moving cosmic antiprotons and antideuterons. Such antinuclei are predicted by a wide variety of allowed dark matter models, as well as other astrophysical theories like primordial black holes.

There are two main components of the GAPS instrument: a large-area tracker and a surrounding time-of-flight system (TOF). The combination of these two systems allows GAPS to effectively differentiate between species of negatively-charged antinuclei and determine the energy deposition, velocity, and trajectory of particles interacting with the detector. This contribution will focus on the TOF, which determines the velocity of the incoming antiparticle and provides the trigger to the experiment. We will give an overview of the TOF detector, an explanation of relevant electronics, and a report on its construction and preliminary performance. The TOF is composed of 160 thin plastic scintillator paddles ranging in length from 1.5 to 1.8 meters. At each paddle end, signals from six silicon photomultipliers are combined to produce two copies of the resulting waveform: one to form the trigger and one for data readout. This design is optimized for low mass and fast data acquisition while still maintaining good light collection.

38th International Cosmic Ray Conference (ICRC2023)
26 July - 3 August, 2023
Nagoya, Japan

*Speaker

PoS(ICRC2023)120

1. Introduction and Science Background

The unknown nature of dark matter (DM) requires investigation with many different experimental strategies. Typically, DM experiments are one of four complementary types: accelerator searches, direct detection, indirect detection, or astrophysical probes. Each of these approaches are optimized for examining the problem of DM from different angles [1]. The General Anti-Particle Spectrometer (GAPS) is an indirect detection experiment which targets cosmic ray (CR) antinuclei as a potential dark matter signature. While anti-particles are not themselves DM candidates, a wide range of existing dark matter models predict antinuclei as a product of DM annihilation or decay [2, 3].

For this reason, CR antinuclei hold important information about the question of dark matter. The Alpha Magnetic Spectrometer (AMS-02) experiment claimed, at one point, to have measured an antiproton flux above expected backgrounds at an energy of around 10 GeV [4]. However, certain aspects of this analysis cast doubt on the reliability of the measurement [5, 6]. The difficulty in fully understanding and disentangling background antiprotons from a potential signal motivates the GAPS search, which will extend to energies below 0.25 GeV per nucleon (an energy range that has yet to be explored by other experiments).

In addition to extending the antiproton sprectrum, the GAPS experiment is searching this energy range for a potential antideuteron flux. There are no known processes which predict antideuteron production at an astrophysical source (also known as primary production). According to conventional physics, CR antideuterons can be produced only through interactions of primary cosmic rays with the interstellar medium (ISM). The minimum energy of an incident particle required for this interaction to produce antideuterons is high, and due to energy conservation the resulting spectra of antideuterons (secondary CRs) are boosted to higher energies, with a very low flux predicted at kinetic energies below 0.5 GeV/n [3].

Theories of antideuteron production beyond the standard model are not constrained by the same kinematic effects. For example, self-annihilation of WIMPs would produce an antideuteron flux significantly above conventional physics backgrounds at low energies.

2. The GAPS Instrument

The GAPS instrument is composed of two main detector components: a large area lithium-drifted silicon tracker (Si(Li)), and the time-of-flight detector (TOF) which surrounds it. Detection and particle identification are accomplished with the following novel technique:

When a negatively charged antiparticle enters the detector volume, it will first interact with and deposit energy in the TOF, which forms the trigger for the experiment. Then, it slows down and is captured by the tracker material, forming a matter-antimatter bound state. This state is extremely unstable, and the decay and annihilation of the exotic atom produces X-rays, pions, and protons which also deposit energy in the tracker and TOF. In particular, the energy of the X-rays are characteristic of the reduced mass of the exotic atom, and can therefore be used to determine the charge-to-mass ratio of the captured particle. The stopping vertex can also be reconstructed from the tracks of annihilation products, leaving us with a full picture of the event.

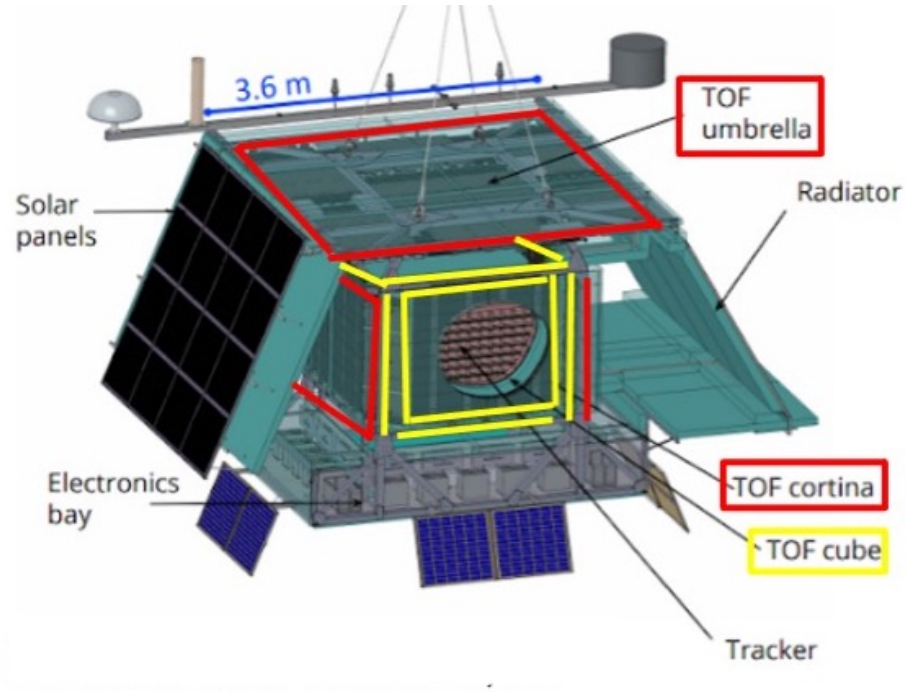

Figure 1: Overview of the GAPS instrument, with the outer TOF highlighted in red and the inner TOF highlighted in yellow.

This technique is optimized for the detection of CR antiparticles with less than 0.25 GeV per nucleon, where antiprotons have never been measured and antideuteron backgrounds are extremely low. This technique is less limited in aperture and mass compared to magnetic spectrometers. With over 7 m^2 of active detector area, the geometric acceptance of GAPS is high, and yet it is light enough to be launched with a long-duration balloon.

2.1 Tracker

The tracker is composed of more than 1000 Si(Li) detectors, each of which is 10 cm in diameter, 2.5 mm thick, and segmented into eight strips. Four of the detectors are grouped together to form a module, which uses an Application Specific Integrated Circuit (ASIC) with 32 channels to provide power and read out data. The modules are arranged in 10 layers with six rows of six modules.

The Si(Li) acts as both a target nucleus for the capture of a negatively charged antiparticle, and as an X-ray detector with a resolution of 4 keV FWHM in the relevant energy range [7, 8]. The operational range of the tracker is around -35° Celsius, which is accomplished with a passive oscillating heat pipe thermal system.

2.2 Time-of-Flight Detector (TOF)

The time-of-flight detector (TOF) is composed of 160 long, thin plastic scintillator paddles ranging in length from 1.5 to 1.8 meters. The paddles are arranged with a slight overlap between adjacent paddles into an inner TOF (the cube, closely surrounding the tracker on all six sides) and the outer TOF (a second layer on top of the cube, called the umbrella, and around the four sides,

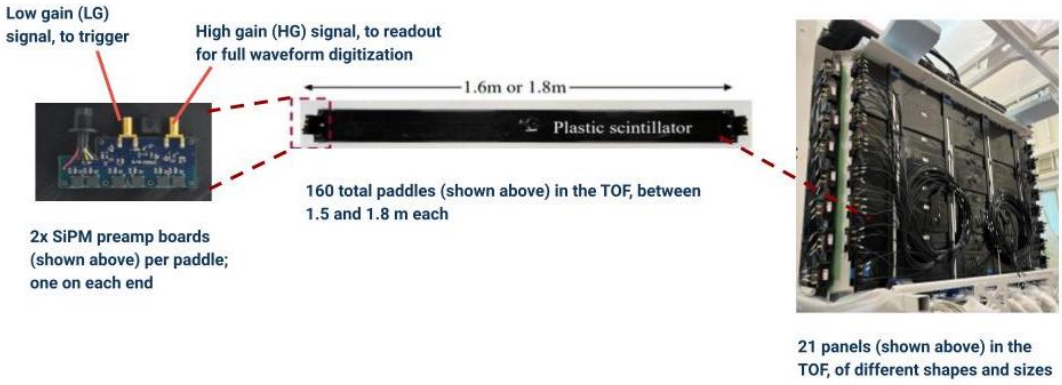

Figure 2: A SiPM preamp, fully wrapped paddle, and mounted TOF panel.

called the cortina). See Figure 1 for a diagram of the experiment with the inner and outer TOFs labeled, and Figure 2 for photos of a TOF paddle and panel.

This arrangement is designed to provide maximum coverage for events inside the tracker, which is significant because the TOF provides the trigger for the experiment; we are able to trigger on, and identify primary tracks for, nearly all particles that stop inside the tracker volume. The TOF is also used to track the out-going annihilation products, which is helpful for particle identification.

3. TOF Construction

The material which comprises the TOF detector area is Eljen EJ-200 general use plastic scintillator. The scintillator was machined by Eljen to have a width of 16 cm, a thickness of 6.35 mm, and lengths varying from 1.5 to 1.8 m. The paddles were wrapped first in aluminum foil and then vinyl blackout material in order to achieve good internal reflection and light-tightness. A small opening was left at the center of the paddle, where a venting tube was inserted in order to allow for outgassing and pressure changes without damage to the wrapping.

Aluminum enclosures were built around each SiPM preamp board, and each board was tested to confirm that all six of the silicon photomultiplier (SiPMs) on the board had a relatively similar gain. For this test, we used an LED, step motor, and darkbox to collect data for 1000 LED flashes in front of each of the six SiPMs. Although the results did not provide an exact gain value, they clearly indicated when one of the SiPMs was non-functional, and they also showed the spread in the response of performance across SiPMs (which was determined to be a measure of the relative gain). Examples of acceptable and unacceptable SiPM responses, depicted with distributions of integrated charge per event, are shown in Figure 3.

When a preamp was shown to have an even response to light pulses across all six SiPMs, it was coupled to the end of a paddle using silicon optical interfaces and optical cement. Two preamps were adhered to each paddle: one on either end. An intricate wrapping procedure was then performed to make the nontrivial geometry of the preamp enclosure light-tight. To confirm light-tightness, the paddle was thoroughly inspected using a flashlight, with a specific focus on the edges of the wrapping material and any difficult corners.

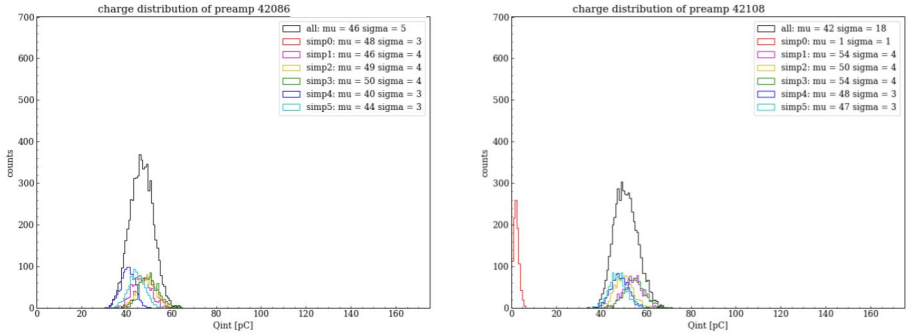

Figure 3: Left: Distribution of integrated charge per event for 6000 events with a well-performing SiPM preamp. Right: Distribution of integrated charge per event for an unacceptable SiPM preamp. Note that one SiPM of the six in the preamp did not have a response to the LED pulse.

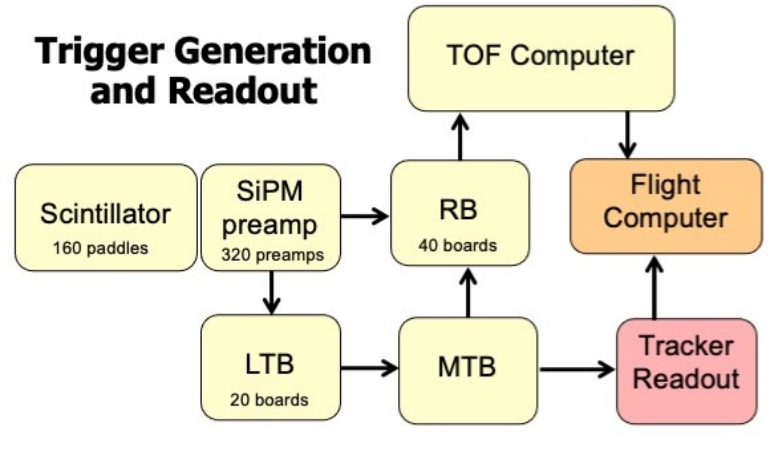

Figure 4: A diagram of the signal pathway for the GAPS trigger generation and readout.

Then, muon calibration data were taken for each paddle to verify that the gains were balanced between paddle ends; this ensures uniform illumination of the paddle. Finally, the paddles were strapped to carbon fiber panels which mounted to the gondola frame of the experiment. The panels are arranged into the inner TOF, which is a *cube* that closely encloses the tracker from all six sides, and the outer TOF, which is composed of the *umbrella* (a single layer above the cube top) and the *cortina* (an additional layer around the four cube sides).

Using the time difference between signals from the same paddle along with the known speed of light in the scintillator material, we are able to determine where along the paddle the particle traversed. This knowledge of the hit location, as well as the information available in the signals themselves (like the total integrated charge and pulse height), will give us information on the trajectory, the velocity (β), and the energy deposited by incoming and outgoing particles. The expected timing resolution for the TOF detector is 400ps.

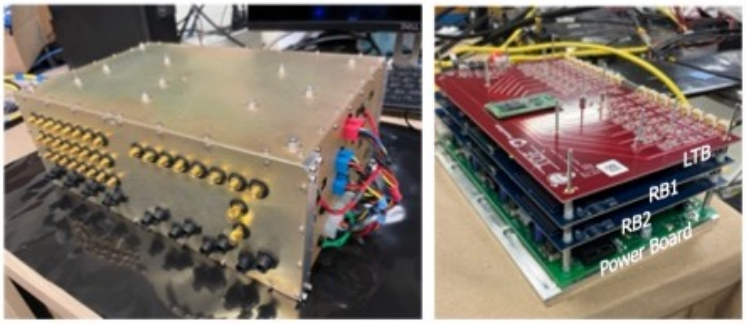

Figure 5: Readout and trigger box, closed (left) and partially disassembled (right) to show the electronics boards within.

4. TOF Electronics

Figure 4 shows the signal pathway for trigger generation and data readout. Each SiPM preamp (two for each of the 160 paddles, for a total of 320 preamps) produces two copies of the signal: a low gain (LG) version and a high gain (HG) version. The LG signal is sent to a local trigger board (LTB), where it is passed through three discriminator levels. The three trigger levels are adjustable, and are currently set to 0.4 min-I (HIT), 2.5 min-I (BETA), and 30 min-I (VETO). HIT is intended to record all paddles with a track in them. BETA is intended to record paddles which have a slow-moving, high-ionizing track. VETO is intended to reject high-Z cosmic ray nuclei, such as Carbon and above. Each LTB encodes the signal from eight paddles using these three trigger levels, and sends a serialized data stream to the master trigger board (MTB) indicating the thresholds reached. There are 20 total LTBs, and the MTB takes the hit pattern from all 20 to make a trigger decision.

The tentative trigger decision requires both the correct energy deposition to trigger BETA but not VETO and a certain number of hits, of any level, in the outer and inner TOFs. If this trigger requirement is met, the MTB generates an event ID which allows for merging events between the TOF readout boards (RBs) and the tracker readout electronics. This event ID is then distributed, along with the trigger decision, to the two systems.

Each of the 40 RBs in the TOF receives eight HG waveform signal from the SiPM preamp and the trigger, event ID, and synchronized clock signal from the MTB. The RBs use the Domino Ring Sampler (DRS-4) ASIC. which samples at a rate of 2 GS/s to digitize a full 512 ns history of the waveforms.

There are 20 readout and trigger (RAT) boxes in the TOF; each RAT box has one LTB, two RBs, and a power board (PB) which accepts 24V battery power and provides power to the three other boards in the RAT box as well as the power and bias voltages to 16 SiPM preamps. See Figure 5 for photos of the inside and outside of the RAT boxes.

5. Prototype and Testing

There have been three stages of prototyping and testing for the GAPS experiment. The first was the GAPS Functional Prototype (GFP) built at MIT Bates Lab in Boston Massachusetts during

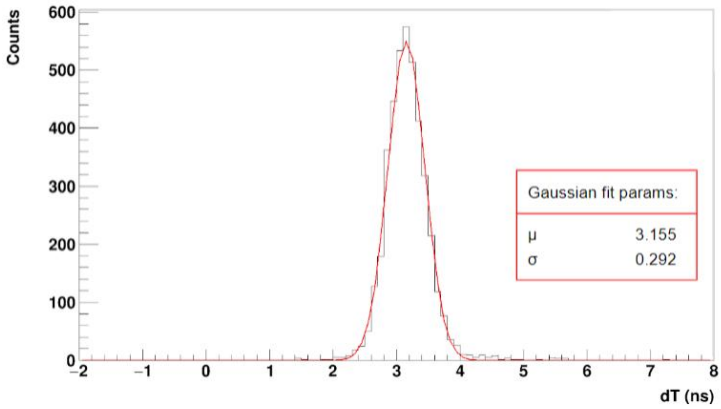

Figure 6: Distribution of times of flight for GFP data for which we find a timing resolution of 290ps based on a Gaussian fit.

the Fall of 2021. The GFP TOF was composed of two parallel panels of twelve 180 cm paddles, separated by a approximately a meter and placed over the GFP tracker. For GFP data taking, we read out data from paddles directly on top of each other using the same RB. We also made cuts on the time difference between paddle ends to select only vertical muons passing through the center of both the upper and lower paddles. With this setup, we were able to verify timing resolution performance (see Figure 6) to 290ps, which is significantly better than our expected resolution of 400ps. This is a significant proof of concept for our design and a good test of our hardware and readout systems.

The next phase of testing started in the fall of 2022, with the integration of the entire tracker with the inner TOF at the UC Berkeley Space Sciences Lab. This ground system testing also involved construction of the mechanical structure. Then, in June 2023, thermal and vacuum performance testing was done at National Technical Systems in El Segundo, CA. The TOF was operated for several hours at float pressure and at both the hottest and coldest temperatures expected in flight from the thermal model. During these operations, the TOF system performed as expected, with the electronic boards working correctly.

6. Conclusion and the Future of GAPS

At the time of this conference, we are pleased to report that the construction of the TOF componented (electronics and hardware) is largely complete, that results from the GFP indicate that we will reach our timing resolution goals, and that the TVAC testing was very successful. Our instrument appears to be robust and prepared for a long-duration balloon launch.

GAPS is currently on schedule to launch during the austral summer of 2024-2025. During fall 2023, the payload will undergo further testing at Nevis Labs, Columbia University. In June of 2024, we will conduct compatibility testing at NASA facilities in Palestine, TX, in preparation for shipment to Antarctica in the fall of 2024.

References

[1] Daniel Bauer, James Buckley, Matthew Cahill-Rowley, Randel Cotta, Alex Drlica-Wagner, Jonathan L. Feng, Stefan Funk, et al. Dark matter in the coming decade: Complementary paths to discovery and beyond. *Physics of the Dark Universe*, 7-8:16–23, mar 2015.

[2] Fiorenza Donato. Antimatter from supersymmetric dark matter. In David B. Cline, editor, *Sources and Detection of Dark Matter and Dark Energy in the Universe*, pages 236–243, Berlin, Heidelberg, 2001. Springer Berlin Heidelberg.

[3] Fiorenza Donato, Nicolao Fornengo, and Pierre Salati. Antideuterons as a signature of supersymmetric dark matter. *Physical Review D*, 62(4), jul 2000.

[4] M. Aguilar, L. Ali Cavasonza, B. Alpat, G. Ambrosi, L. Arruda, N. Attig, S. Aupetit, et al. Antiproton flux, antiproton-to-proton flux ratio, and properties of elementary particle fluxes in primary cosmic rays measured with the alpha magnetic spectrometer on the international space station. *Phys. Rev. Lett.*, 117:091103, Aug 2016.

[5] Jan Heisig, Michael Korsmeier, and Martin Wolfgang Winkler. Dark matter or correlated errors: Systematics of the AMS-02 antiproton excess. *Physical Review Research*, 2(4), oct 2020.

[6] Rebecca K. Leane, Seodong Shin, Liang Yang, Govinda Adhikari, Haider Alhazmi, Tsuguo Aramaki, Daniel Baxter, et al. Snowmass2021 cosmic frontier white paper: Puzzling excesses in dark matter searches and how to resolve them, 2022.

[7] N. Saffold, F. Rogers, M. Xiao, R. Bhatt, T. Erjavec, H. Fuke, C.J. Hailey, M. Kozai, et al. Passivation of si(li) detectors operated above cryogenic temperatures for space-based applications. *Nuclear Instruments and Methods in Physics Research Section A: Accelerators, Spectrometers, Detectors and Associated Equipment*, 997:165015, 2021.

[8] M. Kozai, K. Tokunaga, H. Fuke, M. Yamada, C.J. Hailey, C. Kato, D. Kraych, M. Law, et al. Statistical investigation of the large-area si(li) detectors mass-produced for the gaps experiment. *Nuclear Instruments and Methods in Physics Research Section A: Accelerators, Spectrometers, Detectors and Associated Equipment*, 1034:166820, 2022.

Full Authors List: GAPS Collaboration

T. Aramaki[1], M. Boezio[2,3], S. E. Boggs[4], V. Bonvicini[2], G. Bridges[5], D. Campana[6], W. W. Craig[7], P. von Doetinchem[8], E. Everson[9], L. Fabris[10], S. Feldman[9], H. Fuke[11], F. Gahbauer[5], C. Gerrity[8], C. J. Hailey[5], T. Hayashi[5], A. Kawachi[12], M. Kozai[13], A. Lenni[2,3,14], A. Lowell[7], M. Manghisoni[15,16], N. Marcelli[17,18], B. Mochizuki[7], S. A. I. Mognet[19], K. Munakata[20], R. Munini[2,3], Y. Nakagami[21], J. Olson[22], R. A. Ong[9], G. Osteria[6], K. Perez[23], S. Quinn[9], V. Re[15,16], E. Riceputi[15,16], B. Roach[23], F. Rogers[7], J. L. Ryan[9], N. Saffold[5], V. Scotti[6,24], Y. Shimizu[25], R. Sparvoli[17,18], A. Stoessl[8], A. Tiberio[26], E. Vannuccini[26], T. Wada[21], M. Xiao[23], M. Yamatani[11], K. Yee[23], A. Yoshida[21], T. Yoshida[11], G. Zampa[2], J. Zeng[1], and J. Zweerink[9]

[1]Northeastern University, 360 Huntington Avenue, Boston, MA 02115, USA [2]INFN, Sezione di Trieste, Padriciano 99, I-34149 Trieste, Italy [3]IFPU, Via Beirut 2, I-34014 Trieste, Italy [4]University of California, San Diego, 9500 Gilman Dr., La Jolla, CA 90037, USA [5]Columbia University, 550 West 120th St., New York, NY 10027, USA [6]INFN, Sezione di Napoli, Strada Comunale Cinthia, I-80126 Naples, Italy [7]Space Sciences Laboratory, University of California, Berkeley, 7 Gauss Way, Berkeley, CA 94720, USA [8]University of Hawai'i at Mānoa, 2505 Correa Road, Honolulu, Hawaii 96822, USA [9]University of California, Los Angeles, 475 Portola Plaza, Los Angeles, CA 90095, USA [10]Oak Ridge National Laboratory, 1 Bethel Valley Rd., Oak Ridge, TN 37831, USA [11]Institute of Space and Astronautical Science, Japan Aerospace Exploration Agency (ISAS/JAXA), Sagamihara, Kanagawa 252-5210, Japan [12]Tokai University, Hiratsuka, Kanagawa 259-1292, Japan [13]Polar Environment Data Science Center,Joint Support-Center for Data Science Research,Research Organization of Information and Systems,(PEDSC, ROIS-DS), Tachikawa 190-0014, Japan [14]Università degli Studi di Trieste, Piazzale Europa 1, I-34127 Trieste, Italy [15]INFN, Sezione di Pavia, Via Agostino Bassi 6, I-27100 Pavia, Italy [16]Università di Bergamo, Viale Marconi 5, I-24044 Dalmine (BG), Italy [17]INFN, Sezione di Roma "Tor Vergata", Piazzale Aldo Moro 2, I-00133 Rome, Italy [18]Università di Roma "Tor Vergata", Via della Ricerca Scientifica, I-00133 Rome, Italy [19]Pennsylvania State University, 201 Old Main, University Park, PA 16802 USA [20]Shinshu University, Matsumoto, Nagano 390-8621, Japan [21]Aoyama Gakuin University, Sagamihara, Kanagawa 252-5258, Japan [22]Heliospace Corporation, 2448 6th St., Berkeley, CA 94710, USA [23]Massachusetts Institute of Technology, 77 Massachusetts Ave., Cambridge, MA 02139, USA [24]Università di Napoli "Federico II", Corso Umberto I 40, I-80138 Naples, Italy [25]Kanagawa University, Yokohama, Kanagawa 221-8686, Japan [26]INFN, Sezione di Firenze, via Sansone 1, I-50019 Sesto Fiorentino, Florence, Italy [27]Research and Development Directorate, Japan Aerospace Exploration Agency (JAXA), 2-1-1 Sengen, Tsukuba 305-8505, Japan [28]Research and Development Directorate, Japan Aerospace Exploration Agency, Sagamihara, Kanagawa 252-5210, Japan

This work is supported in the U.S. by the NASA APRA program (Grant Nos. NNX17AB44G, NNX17AB46G, and NNX17AB47G), in Japan by the JAXA/ISAS Small Science Program FY2017, and in Italy by Istituto Nazionale di Fisica Nucleare (INFN) and the Italian Space Agency (ASI) through the ASI INFN agreement No. 2018-22-HH.0: "Partecipazione italiana al GAPS - General AntiParticle Spectrometer." H. Fuke is supported by JSPS KAKENHI grants (JP17H01136, JP19H05198, and JP22H00147) and Mitsubishi Foundation Research Grant 2019-10038. The contributions of C. Gerrity are supported by NASA under award No. 80NSSC19K1425 of the Future Investigators in NASA Earth and Space Science and Technology (FINESST) program. R. A. Ong receives support from the UCLA Division of Physical Sciences. K. Perez and M. Xiao are supported by Heising-Simons award 2018-0766. F. Rogers is supported through the National Science Foundation Graduate Research Fellowship Program under Grant No. 1122374. Y. Shimizu receives support from JSPS KAKENHI grant JP20K04002 and Sumitomo Foundation Grant No. 180322. M. Yamatani receives support from JSPS KAKENHI grant JP22K14065. K. Yee is supported through the National Science Foundation Graduate Research Fellowship under grant 2141064. S. Feldman is supported through the National Science Foundation Graduate Research Fellowship under grant 2034835.